

RESEARCH ARTICLE

An Experimental Machine Learning Approach for Mid-Term Energy Demand Forecasting

SHU-RONG YAN¹, MANWEN TIAN², KHALID A. ALATTAS³,
ARDASHIR MOHAMADZADEH⁴, MOHAMMAD HOSEIN SABZALIAN⁵,
AND AMIR H. MOSAVI^{6,7}

¹School of Business Administration, Hunan University, Changsha 410082, China

²National Key Project Laboratory, Jiangxi University of Engineering, Xinyu 338000, China

³Department of Computer Science and Artificial Intelligence, College of Computer Science and Engineering, University of Jeddah, Jeddah 23890, Saudi Arabia

⁴Multidisciplinary Center for Infrastructure Engineering, Shenyang University of Technology, Shenyang 110870, China

⁵Laboratory of Power Electronics and Medium Voltage Applications (LEMT), The Alberto Luiz Coimbra Institute for Graduate Studies and Research in Engineering (COPPE), Federal University of Rio de Janeiro (UFRJ), Rio de Janeiro 21941-901, Brazil

⁶Obuda University, 1034 Budapest, Hungary

⁷German Research Center for Artificial Intelligence, 66123 Saarbrücken, Germany

Corresponding authors: Ardashir Mohamadzadeh (a.mzadeh@ieee.org) and Amir H. Mosavi (amir.mosavi@kvk.uni-obuda.hu)

This work was supported in part by the Project of the National Science Foundation under Grant 21BJY112, in part by the Fujian Social Science Foundation Project under Grant FJ2021MJDZ045 and Grant FJ2020MJDZ052.

ABSTRACT In this study, a neural network-based approach is designed for mid-term load forecasting (MTLF). The structure and hyperparameters are tuned to obtain the best forecasting accuracy one year ahead. The suggested approach is practically applied to a region in Iran by the use of real-world data sets of 10 years. The influential factors such as economic, weather, and social factors are investigated, and their impact on accuracy is numerically analyzed. The bad data are detected by a suggested effective method. In addition to load peak, the 24-hours load pattern is also predicted, which helps for better mid-term planning. The simulations show that the suggested approach is practical, and the accuracy is more than 95%, even when there are drastic weather changes.

INDEX TERMS Neural networks, machine learning, energy demand, forecasting, artificial intelligence, electrical load, mid-term.

I. INTRODUCTION

With its unique capabilities, electric energy has achieved a privileged position among the types of final energy carriers used by humans. The electricity industry strives to maintain and improve this position in line with the four goals of quality, continuity, cheapness, and environmental compatibility. Because electrical energy cannot be easily stored, production planning from the immediate time horizon of a few seconds to the horizon of tens of years later plays a remarkable role in achieving goals of the electricity industry. Consumers are randomly and with patterns, uniquely connected to the power grid. Seasonal synchronicity in the circuit of chillers or they are connected to the power grid randomly and with specific

The associate editor coordinating the review of this manuscript and approving it for publication was Shadi Alawneh⁸.

behavioral patterns. Seasonal simultaneity in the operation of cooling or heating systems and the simultaneity of all types of household, lighting, public, other, agricultural, and industrial uses form the periodic behavior of the load [1], [2], [3]. In the short-term horizon, the effective parameters include temperature, humidity, cloud cover, wind speed, and time factors such as hours and days of the week. In the long-term horizon, economic and demographic parameters significantly impact the consumption trend. Different forms of load forecasting such as annual, weekly, and daily, are studied [4], [5], [6].

The mid-term forecasting methodologies are suitable for either range of monthly or annual projection. Energy suppliers employ various mid-term forecasting techniques to model the peak of the consumer demand to manage product units optimally and for further scheduling inspection, maintenance

and essential customer service. Consequently, advancing the mid-term energy demand methodologies are essential for better managing and combination of existing power units, controlling the power plants energy conversion as well as improving exchange rates of energy [7], [8], [9].

The scheduling of repairs and maintenance, as well as the efficient use of the power plants, which are closely tied to the reliability, are the primary purposes of MTLF, which has gained significant prominence as a crucial instrument in the last ten years. The MTLF horizon is from several months to 1,2 years [10]. The MTLF assists with resource allocation throughout this time frame and developing various sub-structural components that may be feasible in the mid-term horizon. Mid-term forecasting also aids in improving transmission grid density management, which enhances the system's overall productivity and lowers consumers' energy costs. [11], [12].

Accurate load forecasting is an excellent help for electric companies in production, design, maintenance, service, and distribution units to make the best decision. For this purpose, electricity distribution companies must have prior knowledge of the load demand in the future with high accuracy. Among the factors affecting the load, the pattern is economic factors, time, weather, energy price, sudden disruptions, and other unforeseen factors. Considering the non-linear behavior of load in distribution networks, intelligent methods are a suitable choice for load forecasting, and neural networks are one of these methods. Neural networks are suitable for electricity distribution systems due to their easy implementation and proper performance [13], [14].

In recent decades, many methods have been researched to apply load forecasting. These methods are often different and respond to different engineering and economic analysis theories. One of the essential steps in designing electrical energy distribution systems is to predict the load and its changes since the end of the year required for the design. In addition to saving investment costs, accurate load forecasting also provides the possibility of proper time planning for project implementation. In advanced and developing countries, mid/long terms economic plans are planned to achieve those countries' goals. One of the branches of economic programs is forecasting energy consumption, and its sub-branch is forecasting electric energy consumption. The forecasting of electric energy can provide enough information to design and develop distribution networks [15], [16].

The MTLF using neural networks (NNs) have been also reported in a few studies [17], [18]. For example, in [5] the genetic algorithm is used to train a NN, and the trained NN is applied for MTLF of South Australia. In [19], a price management system is developed by designing a forecasting scheme for load pattern. The wavelet transformation approach is suggested in [20], and its MTLF accuracy is compared with the traditional methods. In [21], a NN is combined with the concept of fuzzy systems, a nested tree learning scheme is developed for optimizing, and it is compared with other local NN models. The impact of weather factors on MTLF has

been entirely investigated in [22]. To predict the load, a set of data is needed as input so that the predictive model can predict the future load of the system based on them. The selection of these inputs can be done experimentally or by intelligent systems. These inputs can be done experimentally or by intelligent systems [7], [23].

The main feature of NNs is learning the complex relationship between inputs and output vectors, which is very difficult to achieve in old algorithmic methods. The past values of the load along with other related information are given to the NN as inputs and the output of NN is the expected predicted value [24], [25]. This action can be done by establishing an internal non-linear relationship between the input/output signals automatically by NN and performing the prediction by it in the next steps. A very important aspect of NNs is the updating of the parameters of NNs during the working phase adaptively and automatically [15], [26], [27]. The manifold learning scheme is developed in [28] for MTLF, the computations are simplified, and the suggested approach is examined by the use of data sets of New England. Fuzzy systems have recently received attention in the problem of load estimation due to their ability to formulate and use experiences and experts' unconscious knowledge. The superiority of such systems is the use of the experience of experts and, as a result, more appropriate performance in specific conditions, and on the other hand, due to the lack of training and regulation, they usually have lower accuracy. Suppose it is possible to prepare the training phase, similar to what is used in NNs, to minimize the error of the fuzzy system prepared by experts. In that case, the load estimation will be done with better accuracy [15], [29]. Also, NNs are combined with the concepts of fuzzy systems to enhance the accuracy of modeling [30], [31], [32].

In current study, a practical direction is presented to mid-term load forecast. The first step is to detect any relation between variables. In the next step, the most effective variables are determined. Finally, further optimizations are applied on the designed scheme to get the best accuracy. The forecasting strategy is identifying the pattern of load peak with optimized NN, and using optimized NN for forecasting. The mid-term forecasting horizon is considered one year ahead. The main contributions are summarized as:

- This paper proposes an experimental approach for MTLF. All details are presented step-by-step in details.
- The suggested machine learning technique is simple and effective. It can be employed to real-world problems.
- A practical technique is presented to select the influential variables.
- To improve the accuracy, a simple method is suggested to train the suture of NN.
- A simple approach is suggested to analyze the effect of various economic, social, and climate variables.

II. THE CORRELATION AMONG THE VARIOUS VARIABLES

Various computational approaches can measure the dependence or relationship between two signals. The meaning of

the correlation coefficient between two signals is the prediction ability of one signal in terms of the other. For example, supply and demand are two interdependent phenomena. One of the methods of representing the relationship between two signals is to compute “Covariance” or “Correlation Coefficient” between them. The larger the value of these two indices, the greater the relationship or dependence between the two variables. For example, we can consider a substantial dependence between electricity consumption and air temperature variables. Because as the temperature increases, the use of cooling devices also increases electricity consumption. As a result, there is an excellent dependence between these two variables. Of course, it should be noted that covariance or correlation does not indicate the cause-and-effect relationship but is only a measure to show the rate of dependence between two signals.

The data correlation and scatter diagram are used as one of the standard methods for the general investigation of the relationship among data. The correlation value is between -1 and 1 . This coefficient has two sections: the scalar value and the sign. The scalar value shows how strong the linear relationship between two variables is. The sign shows the direction of this relationship is positive or negative. The relationship of the Pearson correlation coefficient is as follows [33]:

$$r_{xy} = \frac{s_{xy}}{s_x s_y} \quad (1)$$

where,

$$s_{xy} = \frac{\sum (x_i - \bar{x})(y_i - \bar{y})}{n - 1} \quad (2)$$

where, n indicates sample numbers. If the correlation is positive, it means that a rising in another variable accompanies a rising in one variable. Also, the decrease in a variable is accompanied by a decrease in another variable. The closer to 1 , the correlation is, the more significant the relationship between the two factors. On the contrary, the correlation coefficient close to zero shows a weak linear relationship. In this case, if the scatter diagram of two variables is plotted, it seems that the points are randomly plotted in the plane. Of course, it should be noted that if there is a non-linear relationship, the correlation coefficient can still be about zero, indicating no linear relationship between them. In other words, a zero correlation coefficient shows only the absence of a linear relationship between the two variables but being independent of the two variables cannot be the result. When the Pearson correlation coefficient is zero between two variables, these variables are independent of each other only in case of the distribution of variables is normal.

Following, the scatter diagram between the load peak variables and other variables such as temperature average, temperature peak, low limit temperature, the number of electricity subscribers, Gross Domestic Product, and the rate of inflation is depicted.

A. THE CORRELATION DIAGRAMS BETWEEN TOTAL LOAD PEAK AND AVERAGE TEMPERATURE

The temperature, humidity, the sky cloudy amount, and wind speed affect intensely the behavioral pattern of short-term load. The experience has shown that weather conditions have a high correlation with the consumption rate of electric load, especially the weather temperature. To state the intensity of this correlation, it can be said with confidence that by considering the load curves in limited duration, only with weather inputs, the short-term load can be forecasted with great accuracy and the forecast accuracy can be raised by entering the other effective factors. The season changes affect directly the consumption rate. For example, in different seasons according to the reopening or closure of educational centers like schools and universities or concerning the change of daylight hours and etc., the consumption pattern will be changed from one season to another season [34], [35].

The electricity consumption pattern of Iranian families changing the seasons has many changes due to using of different appliances. In the warm seasons by using cooling appliances (like a cooler) that have high power and also a long consumption time, many loads are imposed on the grid, as there are always the most problems in terms of peak hours of power consumption from mid-July to mid-September and especially at hours between 19 to 23. In the cold seasons, we will see an increase in consumption by entering heating devices like electric heater that also has high power and is used for continuous hours. Also, the electricity consumption pattern is different considering the various climate and cultural conditions in the different areas of the country. In general, due to the wide use of cooling devices, the tropical regions compared to other regions of the country have more power consumption in summer.

In this part, on the one hand, the correlation and scatter diagrams are plotted between nightly and daily total load peaks, and on the other hand, the average, low limit, and high limit of the country’s absolute temperature. The temperature is a very significant factor in changes in country load. These changes are related to seasonal changes and heating and cooling device replacement. The correlation diagram of the high daily temperature limit and the daily total load peak of the whole country is shown from 2007 to 2017 in figure 1. The correlation diagram of a low daily temperature limit and a daily total load peak of the whole country is shown from 2007 to 2017 in figure 2. The correlation diagram of daily average temperature and the country’s daily total load peak from 2007 to 2017 is depicted in figure 3. Figure 4 shows the correlation diagram of the high daily temperature limit and the country’s nightly load peak from 2007 to 2017. The correlation diagram of a low daily temperature limit and a nightly load peak of the whole country is shown from 2007 to 2017 in figure 5. Figure 6 shows the correlation diagram of daily average temperature and the entire country’s nightly load peak from 2007 to 2017. The correlation diagram of the annual average of high-temperature limit and load peak yearly average of the whole country is shown

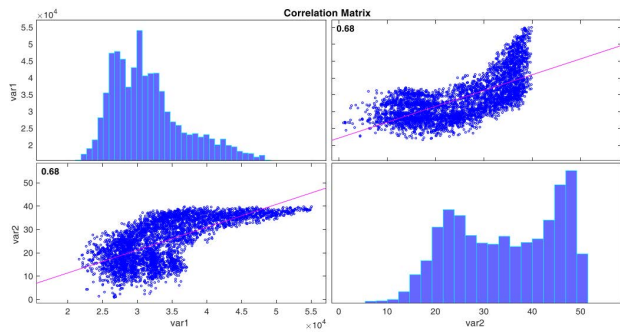


FIGURE 1. The correlation trajectory of daily temperature peak and daily load peak.

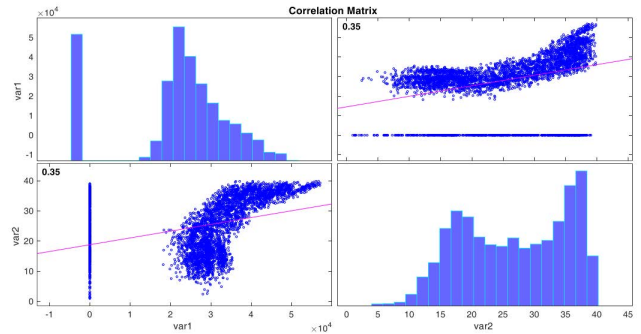


FIGURE 4. The correlation trajectory of high daily temperature limit and nightly load peak.

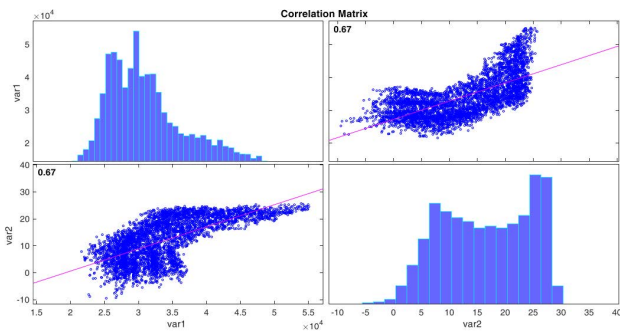


FIGURE 2. Correlation trajectory of low daily temperature limit and daily load peak.

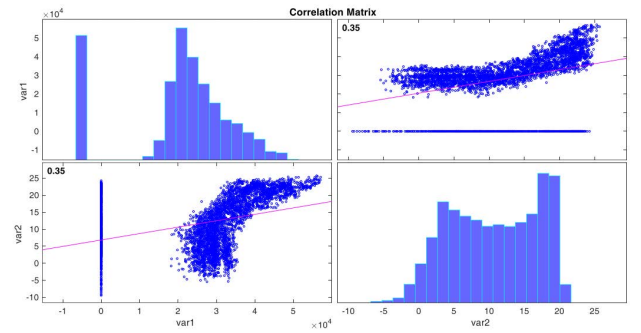


FIGURE 5. The correlation trajectory of low daily temperature limit and nightly load peak.

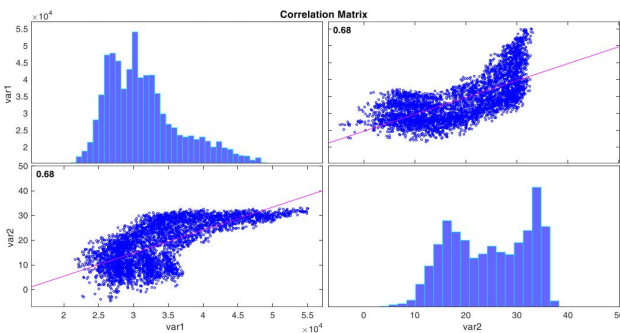


FIGURE 3. The correlation trajectory of daily average temperature and daily load peak.

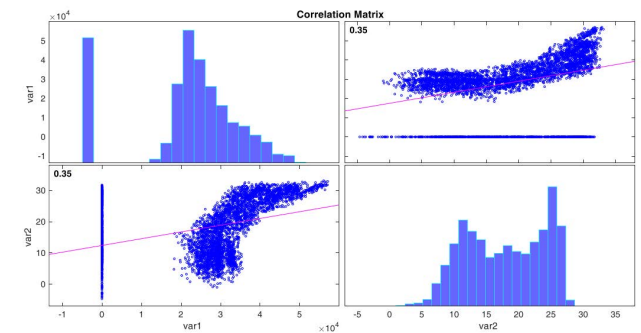


FIGURE 6. The correlation trajectory of daily average temperature and nightly load peak.

from 2007 to 2017 in figure 7. The correlation diagram of a yearly average of temperature low limit and load peak annual average of the whole country is shown from 2007 to 2017 in figure 8. The correlation diagram of the country's yearly average temperature and load peak annual average is shown from 2007 to 2017 in figure 9. We see a considerable correlation between temperature and load. Also, a high correlation between the yearly average temperature and load can be seen.

B. THE CORRELATION DIAGRAM BETWEEN THE TOTAL LOAD PEAK AND VARIABLE GDP

Gross domestic product (GDP) is essential for macroeconomic indicators because it is the most significant economic

performance index in analysis and assessments. The total Rial value of the final productions produced by monetary units residing in the country in a specific period (annually or seasonal) is called GDP. Each product produced in the economy takes several steps to become the final product. For example, as a final product directly consumed, bread goes through stages like wheat and flour production. The stage number of conversion or fabrication in complex industrial products is more. However, in estimating the GDP, the final product value (bread) must be used because the flour worth is hidden in it, as the wheat value is implicitly present in flour. If we consider the value of each of these steps in GDP separately, we have overestimated the value of products produced in the economy.

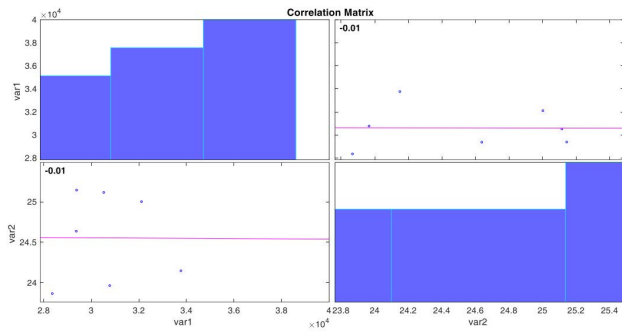


FIGURE 7. The correlation trajectory of annual average of high temperature limit and annual average of total load peak.

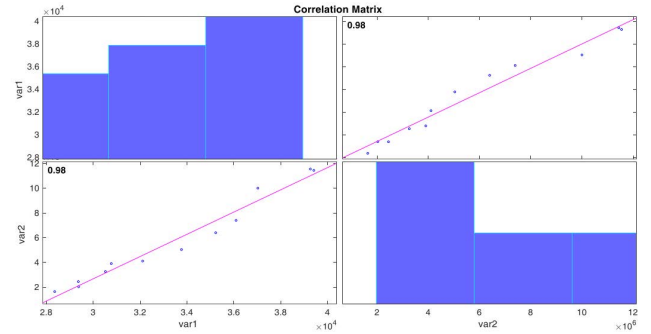


FIGURE 10. The correlation trajectory of the annual average of daily load peak of whole country and GDP variable.

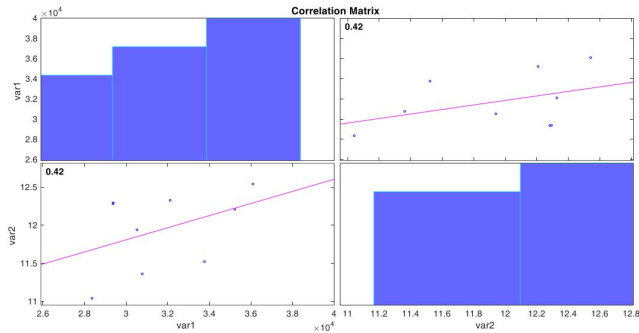


FIGURE 8. The correlation trajectory of the annual average of low temperature limit and annual average of total load peak.

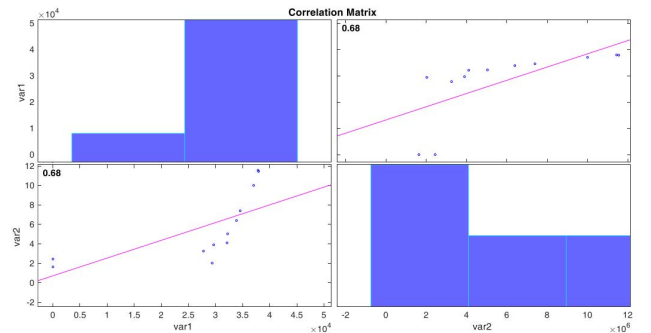


FIGURE 11. The correlation trajectory of the annual average of nightly load peak.

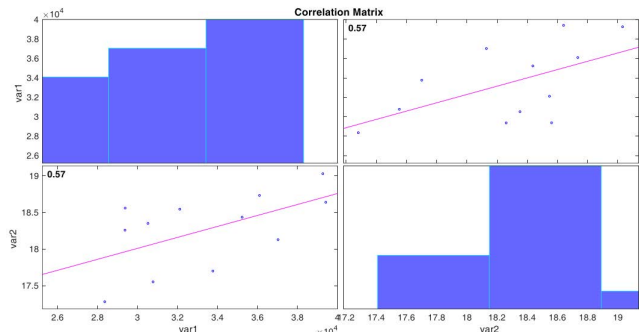


FIGURE 9. The correlation trajectory of the annual average of temperature and annual average of daily total load peak.

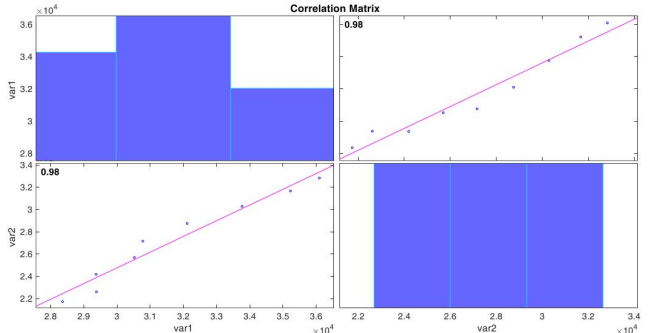


FIGURE 12. The correlation trajectory of the daily load peak of whole country and the number of subscribers.

For this reason, the final word has been emphasized in the definition above. A country’s GDP index is considered the influential variable in changes in load in various references. The correlation diagram between the annual average of the whole country’s daily and nightly load peak and the GDP index from 2007 to 2017 is given in figures 10 and 11. A high correlation is seen between the GDP index and the annual average load peak due to the industrial and residential energy consumption growth as a result of economic development.

C. THE CORRELATION DIAGRAM BETWEEN LOAD PEAK AND THE NUMBER OF SUBSCRIBERS

One of the significant and influential factors in changes in load is the population changes index or the changes index of

the number of subscribers. They are considering that nearly 80% of the numbers of subscribers are household subscribers. So, the changes in the number of subscribers considerably affect the load changes of the whole country. The correlation diagrams between the annual average of the country’s daily and nightly load peak are given in figures 12- 13. As can be seen, there is a high correlation between the number of subscribers and the load peak.

D. THE CORRELATION DIAGRAMS BETWEEN THE INFLATION RATE AND LOAD PEAK

The price index of consumer goods and services (CPI) is a measure criterion of changes in the price of goods and

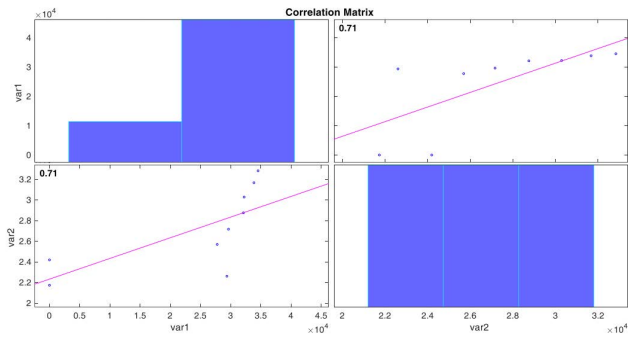


FIGURE 13. The correlation of the total average of nightly load peak and the number of subscribers.

services consumed by Iranian urban households. As a tool for measuring the typical cost of goods and services consumed by households, this index is one of the best criteria for measuring the change in money in the country. The monthly inflation rate is obtained by calculating the percentage change of the average CPI index in 12 months ending up to the desired month compared to the same period of the past year. It is evident if the considered month is March, it is called the inflation rate of the supposed year. The correlation diagram between the annual average daily and nightly load peak of the whole country and the annual inflation rate (from 2007 to 2017) is depicted in figures 14 and 15. The figures show a medium correlation between the annual average of daily load peak and the annual inflation rate. As expected, the load peak will be reduced by increasing inflation, decreasing the life level, and reducing the purchasing power. Also, by increasing inflation, some industries are influenced because one of the main reasons for rising inflation in our country is the direct sanction that affects the industry.

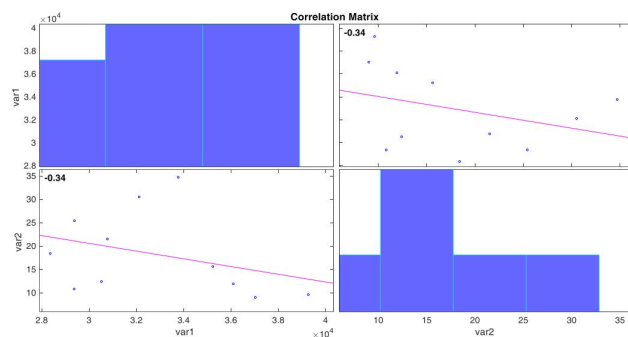


FIGURE 14. The correlation of annual average of daily load peak of whole country and annual inflation rate.

E. THE CORRELATION DIAGRAM BETWEEN THE GROSS PRODUCT OF ELECTRICITY AND CONSUMPTION LOAD

One of the goals of long-term load peak forecasting is appropriate investment in power generation. This section plots the correlation diagrams of the gross product of the entire country’s power with the annual load peak. These diagrams are shown in figure 16 and figure 17 As it can be seen, a good

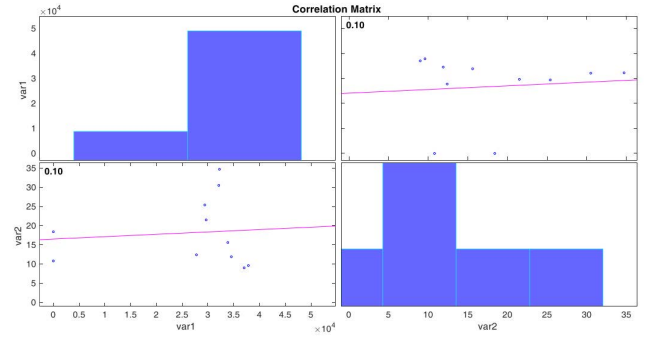


FIGURE 15. The correlation of annual average of nightly load peak of whole country and annual inflation rate.

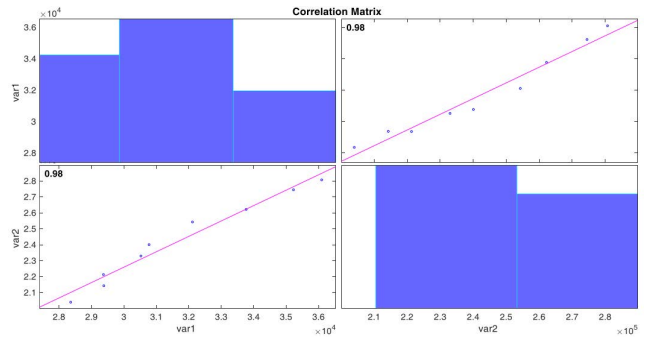


FIGURE 16. The correlation of annual average of daily load peak of whole country and gross product of electricity.

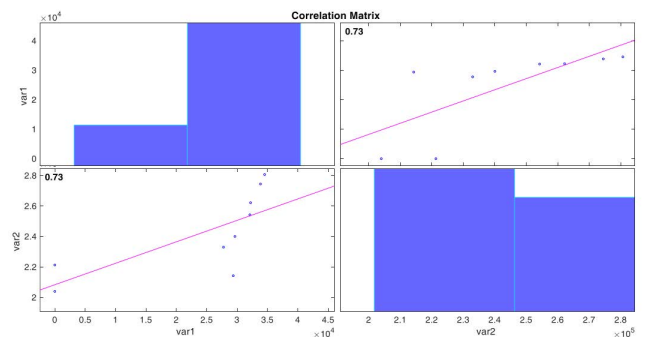


FIGURE 17. The correlation of annual average of nightly load peak of whole country and gross product of electricity.

investment has been made in generating electricity during the last 12 years, and production has grown, corresponding to the increase in consumption.

III. DETERMINING THE EFFECTIVE VARIABLES AND REPRESENTING THE PROPOSED METHOD AND INVESTIGATING THE RESULTS

In this report, firstly, the influence of various variables on MTLF is examined. For this purpose, in various scenarios, the inputs of the NN are changed, and the rate of forecast error of load peak is examined to check which group of inputs has the better results in the forecast. The accuracy

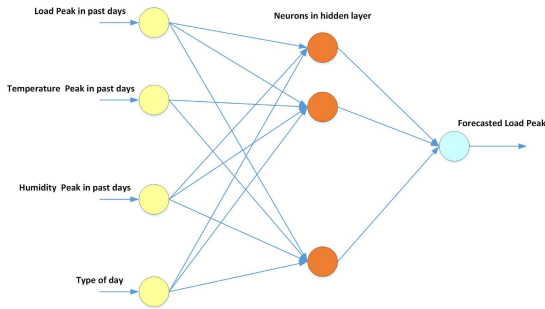


FIGURE 18. A general view on the suggested NN.

models are shown in various diagrams. The data is used for learning from 2007 to 2017, and the data from 2018 to 2020 is used for tests. After determining the adequate inputs, the structure optimization (number of neurons), the learning method optimization, and the effect of undesired inputs are investigated. In this section, the influential variables in load forecasting are investigated.

A. INITIAL MODEL

To find the influential variables in regarded issues, the best-proposed method is that each of the variables is applied in various scenarios as input to the regarded model, and the effect of each must be investigated separately. The same model and educational method are considered, and the model’s inputs are examined in various scenarios. The inputs of the desired model are considered as follows:

- Consumption load in one past year
- Consumption load in 2 past years
- Consumption load in 3 past years
- Consumption load in 4 past years
- Consumption load in 5 past years
- GDP rate in one past year
- GDP rate in 2 past years
- GDP rate in 3 past years
- GDP rate in 4 past years
- GDP rate in 5 past years
- Average temperature in one past year
- Average temperature in 2 past years
- Average temperature in 3 past years
- Average temperature in 4 past years
- Average temperature in 5 past years
- The inflation rate in one past year
- The number of electricity subscribers in the one past year
- The day type of week

B. TRAINING THE PROPOSED MODEL

A neural network (NN) structure with two active layers is considered (see figure. 18). The number of n_0 and n_2 neurons in the first active layer and in the second active layer are considered. As a result, the weights related to the active neurons in these two layers are as follows respectively:

First layer:

$$\begin{cases} w_{10}^1, w_{11}^1, w_{12}^1, \dots, w_{1n_0}^1 \\ w_{20}^1, w_{21}^1, w_{22}^1, \dots, w_{2n_0}^1 \\ \cdot \\ \cdot \\ w_{n_1 0}^1, w_{n_1 1}^1, w_{n_1 2}^1, \dots, w_{n_1 n_0}^1 \end{cases} \quad (3)$$

For second layer:

$$\begin{cases} w_{10}^2, w_{11}^2, w_{12}^2, \dots, w_{1n_1}^2 \\ w_{20}^2, w_{21}^2, w_{22}^2, \dots, w_{2n_0}^2 \\ \cdot \\ \cdot \\ w_{n_2 0}^2, w_{n_2 1}^2, w_{n_2 2}^2, \dots, w_{n_2 n_0}^2 \end{cases} \quad (4)$$

The relationships of weighted inputs with bias in the neurons of first active layer are as follows:

$$\begin{cases} neuron_1^1 \Rightarrow net_1^1 = w_1^1 \cdot x + b_1^1 \\ neuron_2^1 \Rightarrow net_2^1 = w_2^1 \cdot x + b_2^1 \\ \cdot \\ \cdot \\ neuron_{n_1}^1 \Rightarrow net_{n_1}^1 = w_{n_1}^1 \cdot x + b_{n_1}^1 \end{cases} \quad (5)$$

Also, the relationships of weighted inputs with bias in the neurons of second active layer are as follows:

$$\begin{cases} neuron_1^2 \Rightarrow net_1^2 = w_1^2 \cdot o^1 + b_1^2 \\ neuron_2^2 \Rightarrow net_2^2 = w_2^2 \cdot o^1 + b_2^2 \\ \cdot \\ \cdot \\ neuron_{n_2}^2 \Rightarrow net_{n_2}^2 = w_{n_2}^2 \cdot o^1 + b_{n_2}^2 \end{cases} \quad (6)$$

Which finally, the outputs of the first and second active layers are as follows:

$$o_j^1(k) = f^1 [net_j^1(k)]$$

$$net_j^1 = \sum_{i=0}^{n_0} w_{ji}^1(k)x_i^1(k) + b_j^1(k) \quad (7)$$

$$o_k^2(k) = f^2 [net_k^2(k)],$$

$$net_k^2 = \sum_{j=0}^{n_1} w_{kj}^2(k)o_j^1(k) + b_k^2(k) \quad (8)$$

The loss function to train NN is the squared error between the real and estimated signals. The main focus of current study is to present a practical MTLF approach. So, it is tried to use more effective and straightforward methods. The extended Kalman filter (EKF) results in reasonable accuracy with good resistance against noisy data. For training the

parameters of the second layer based on EKF, the following relationships are used:

$$w^2(k) = w^2(k - 1) + p_o(k)\varphi_o(k)(e_{o1}(k)) \quad (9)$$

where, e represents the error between real and estimated signals, and [36]

$$p_o(k) = p_o(k - 1)[I - K_o(k)H_o(k)] + Q_o(k) \quad (10)$$

$$K_o(k) = \frac{p_o(k - 1)H_o^T(k)}{R_o(k) + H_o(k)p_o(k - 1)H_o^T(k)} \quad (11)$$

And $H_o(k)$ is implemented as following form:

$$H_o(k) = \frac{\partial o^2(k)}{\partial net^2(k)} \frac{\partial net^2(k)}{\partial w^2(k)} = f'^2(k)o^1(k) \quad (12)$$

The learning rules of the first layer parameters are:

$$\Delta w^1(k) = \eta_w \delta^1(k) \cdot o^0(k) \quad (13)$$

$$\Delta b^1(k) = -\eta_b \cdot \frac{\partial E(k)}{\partial b^1(k)} \quad (14)$$

where, its chain law is as follows:

$$-\eta_b \cdot \frac{\partial E(k)}{\partial e(k)} \cdot \frac{\partial e(k)}{\partial o^2(k)} \frac{\partial o^2(k)}{\partial net^2(k)} \frac{\partial net^2(k)}{\partial o^1(k)} \frac{\partial o^1(k)}{\partial net^1(k)} \frac{\partial net^1(k)}{\partial b^1(k)} \quad (15)$$

$$\Delta b^1(k) = \eta_b e(k) \cdot f'^2(k) \cdot w^2(k) \cdot f'^1(k) \quad (16)$$

$$\Delta b^1(k) = \eta_b \delta^1(k) \quad (17)$$

where,

$$\delta^1(k) = e(k) \cdot f'^2(k) \cdot w^2(k) \cdot f'^1(k) \quad (18)$$

C. INVESTIGATING THE EFFECT OF VARIOUS VARIABLES

The various influential variables are considered as inputs in different intervals, and the effect of each of these inputs is evaluated in various scenarios. To make a better comparison, neural structure (number of neurons) and learning algorithm coefficient should be noted. The number of training iterations is considered the same for all states. After finding adequate input sets, the neurons and learning algorithm will also be optimized. The data from the year 2007 to the year 2017 has been used as training data, and from early 2018 to the end of September 2019, used as test data. The data will be available upon request. The gradient descent and Extended Kalman filter have been used for training NN. All input data of NN has been normalized between 0 and 1. To do this, all data is divided by its maximum value. The general views on the time series of load, temperature, and humidity are depicted in figures 19- 21.

In any scenario, the training is iterated 10 times and the maximum, minimum, and average percentage error along with the test and training diagrams are presented to evaluate. To evaluate, the mean absolute percentage error (MAPE) criterion is used that is defined as follow:

$$\frac{1}{n} \sum_{t=1}^n \left| \frac{A_t - F_t}{A_t} \right| \times 100 \quad (19)$$

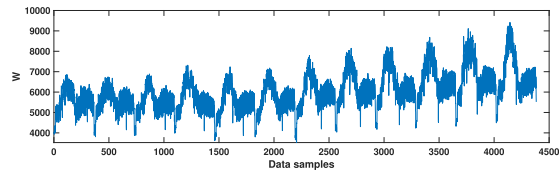


FIGURE 19. The time series of load peak.

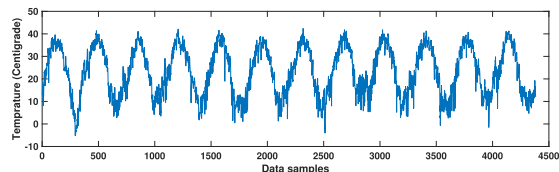


FIGURE 20. The time series of temperature peak.

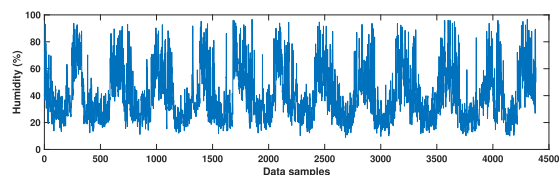


FIGURE 21. The time series of humidity peak.

TABLE 1. MAPE results for test and training data-scenario 1.

	Average (%)	Minimum	Maximum
	(%)	(%)	(%) (%)
Test data	20.6763	11.3341	42.7352
Training data	8.1363	7.4233	9.1669

TABLE 2. MAPE results for test and training data-scenario 2.

	Average (%)	Minimum	Maximum
	(%)	(%)	(%) (%)
Test data	13.2312	11.0410	16.4246
Training data	7.7036	7.0100	8.9069

In which, A_t is the target and real data, F_t is estimated data, and n denotes the data number.

1) THE FIRST SCENARIO

In this scenario, the neural inputs are considered as the load, GDP and maximum temperature, and day type in terms of being holiday or non-holiday. The results obtained for MAPE are given in Table 1.

2) SCENARIO 2

In this scenario, the neural inputs are considered as the peaks of load, humidity, and temperature on the same day in the last four years, and the day type. In this scenario, only the weather conditions and data are inputs. The purpose is to study the effect of omitting economic variables. The results obtained for MAPE are given in Table 2. As it can be seen, the omitting of economic variables improves the results.

TABLE 3. MAPE results for test and training data-scenario 3.

	Average (%) (%)	Minimum (%)	Maximum (%) (%)
Test data	15.0881	13.4854	17.4616
Training data	7.5173	7.1548	8.4785

TABLE 4. MAPE results for test and training data-scenario 4.

	Average (%) (%)	Minimum (%)	Maximum (%) (%)
Test data	12.7462	10.7337	14.4736
Training data	7.4734	7.0476	8.6475

TABLE 5. MAPE results for test and training data-scenario 5.

	Average (%) (%)	Minimum (%)	Maximum (%) (%)
Test data	14.8584	12.7918	19.0140
Training data	7.2440	6.8626	7.7674

3) SCENARIO 3

In this scenario, the neural inputs are considered as the load peak, the average temperature on the same day in the last four years, and the day type. Compared with the previous scenario, the average temperature is used instead of the temperature peak, and the humidity variable is eliminated. The results obtained for MAPE are given in Table 3. As seen, using the average temperature instead of the temperature peak and omitting the humidity variable has worsened the results. In the following scenario, the direct effect of temperature peak is investigated.

4) SCENARIO 4

In this scenario, the neural inputs are the load, and maximum temperature on the same day in the last four years, the day type. Compared with the previous scenario, the temperature peak is used instead of the average temperature. The aim is to study the direct effect of temperature peaks. The results obtained for MAPE are given in Table 4. As can be seen, using the temperature peak instead of the average temperature improves the results.

5) SCENARIO 5

In this scenario, the neural inputs are considered as the peaks of load and temperature, and least temperature on the same day in the last four years, and the day type. Compared to the previous scenario, the minimum temperature has also been used. The results obtained for MAPE are given in Table 5. As can be seen, adding the minimum temperature variable has made the results worse.

6) SCENARIO 6

In this scenario, the neural inputs are the GDP, and inflation rate in the last four years, the maximum temperature on the same day in the last four years, and the day type. The load

TABLE 6. MAPE results for test and training data-scenario 6.

	Average (%) (%)	Minimum (%)	Maximum (%) (%)
Test data	22.3049	14.5328	35.4105
Training data	9.7460	9.3455	10.3082

TABLE 7. MAPE results for test and training data-scenario 7.

	Average (%) (%)	Minimum (%)	Maximum (%) (%)
Test data	11.1103	10.3145	12.7135
Training data	7.7222	7.3564	8.9116

TABLE 8. MAPE results for test and training data-scenario 8.

	Average (%) (%)	Minimum (%)	Maximum (%) (%)
Test data	13.6296	11.9973	14.6719
Training data	7.1738	7.0100	7.5292

peak is eliminated in this scenario, and only the economic and weather variables are considered. The aim is to examine the effect of load patterns on forecast accuracy. The results obtained for MAPE are given in Table 6. As can be seen, the elimination of the load peak variable in the previous times has worsened the results. This investigation shows that using the changes pattern of load peak helps increase forecast accuracy significantly.

7) SCENARIO 7

In this scenario, the neural inputs are as follows, The average of temperature and load peaks in the same month of the old years, the load/temperature peaks on the same day of the past years, the month No., the day No., the day type. The results obtained for MAPE are given in Table 7.

8) SCENARIO 8

In this scenario, the neural inputs are as follows, The load peak on the same day of last four years, and the mediocre load peak in the same month of last four years. The results obtained for MAPE are given in Table 8.

9) SCENARIO 9

In this scenario, the neural inputs are as follows, The peaks of load and temperature, mediocre peaks of load and temperature on the same day of last four years, mediocre peaks of load and temperature in the last four years, and weekdays. The results obtained for MAPE are given in Table 9.

10) SCENARIO 10

In this scenario, the neural inputs are as follows: The load peak on the same day of last four years, the mediocre load peak in the same month of last four years, the average load peak in the last four years, and the day of the week. The results obtained for MAPE are given in Table 10.

TABLE 9. MAPE results for test and training data-scenario 9.

	Average (%) (%)	Minimum (%)	Maximum (%) (%)
Test data	16.0681	13.4045	20.3604
Training data	10.3920	8.4624	11.9720

TABLE 10. MAPE results for test and training data-scenario 10.

	Average (%) (%)	Minimum (%)	Maximum (%) (%)
Test data	18.0604	16.0230	19.7469
Training data	7.1492	6.7648	7.9516

TABLE 11. MAPE results for test and training data-scenario 11.

	Average (%) (%)	Minimum (%)	Maximum (%) (%)
Test data	11.6335	10.5074	13.8702
Training data	7.2497	6.9044	8.5408

TABLE 12. MAPE results for test and training data-scenario 12.

	Average (%) (%)	Minimum (%)	Maximum (%) (%)
Test data	15.4639	11.8316	17.9435
Training data	8.8849	8.4286	9.2520

11) SCENARIO 11

In this scenario, the neural inputs are as follows, The load peak on the same day of last four years, the mediocre temperature peak in the same month of last four years, and the weekday. The results obtained for MAPE are given in Table 11.

12) SCENARIO 12

In this scenario, the neural inputs are as follows: The load/temperature peaks on the same day of last four years, the average peaks of load and temperature in the same month in the last four years, and weekday. The results obtained for MAPE are given in Table 12.

13) SCENARIO 13

In this scenario, the neural inputs are as follows: The peaks of load and temperature on the same day in the last four years, the average peaks of load and temperature in the same month in the last four years, and weekday. The results obtained for MAPE are given in Table 13.

14) SCENARIO 14

The maximum load on the same day of last four years is divided by the mediocre maximum load of same year, maximum temperature of the same day is divided by the mediocre temperature on the same month in the last four

TABLE 13. MAPE results for test and training data-scenario 13.

	Average (%) (%)	Minimum (%)	Maximum (%) (%)
Test data	10.8772	9.7480	12.5317
Training data	8.6243	8.2844	8.9775

TABLE 14. MAPE results for test and training data-scenario 14.

	Average (%) (%)	Minimum (%)	Maximum (%) (%)
Test data	16.0447	14.6837	17.9241
Training data	10.8354	10.3087	12.0298

TABLE 15. MAPE results for test and training data-scenario 15.

	Average (%) (%)	Minimum (%)	Maximum (%)
Test data	20.4217	15.4630	25.0128
Training data	12.0868	10.9364	13.4835

TABLE 16. MAPE results for test and training data-scenario 16.

	Average (%) (%)	Minimum (%)	Maximum (%)
Test data	12.7718	11.6834	13.7283
Training data	6.9026	6.7852	7.0408

years, and weekday. The results obtained for MAPE are given in Table 14.

15) SCENARIO 15

In this scenario, the neural inputs are as follows: GDP, NOS, temperature peak, inflation rate in the last four years, and weekdays. In this scenario, the load peak data has been eliminated. The results obtained for MAPE are given in Table 15. As it can be seen, eliminating the load peak data in the past years has made the results worse.

16) SCENARIO 16

In this scenario, the neural inputs are as follows: The load peak in the last four years is a weekday. In this scenario, the weather, economic, and population data are eliminated. The results obtained for MAPE are given in Table 16. As it can be seen, eliminating the weather data, economic data, and population data has not considerably affected the performance. To justify this issue, it should be noted that when the load peak in the past years is considered input, other influential factors have also been indirectly involved.

D. GENERAL COMPARISON OF SCENARIOS

In this section, the obtained results in the previous section are summarized. All obtained results are presented in Table 17 for test data and Table 18 for train data.

TABLE 17. The summary of obtained results for MAPE-test data.

Scenario No	Average (%)	Min (%)	Max (%)
1	20.6763	11.3341	42.7352
2	13.2312	11.0410	16.4246
3	15.0881	13.4854	17.4616
4	14.4736	10.7337	12.7462
5	14.8584	12.7918	19.0140
6	22.3049	14.5328	35.4105
7	11.1103	10.3145	12.7135
8	13.6296	11.9973	14.6719
9	16.0681	13.4045	20.3604
10	18.0604	16.0230	19.7469
11	11.6335	10.5074	13.8702
12	15.4639	11.8316	17.9435
13	10.8772	9.7480	12.5317
14	16.0447	14.6837	17.9241
15	20.4217	15.4630	25.0128
16	12.1277	16.9411	13.4688

TABLE 18. The summary of obtained results for MAPE-train data.

Scenario No	Average (%)	Min (%)	Max (%)
1	8.1363	7.4233	9.1669
2	7.7036	7.0100	8.9069
3	7.5173	7.1548	8.4785
4	7.4734	7.0476	8.6475
5	7.2440	6.8626	7.7674
6	9.7460	9.3455	10.3082
7	7.7222	7.3564	8.9116
8	7.1738	7.0100	7.5292
9	10.3920	8.4624	11.9720
10	7.1492	6.7648	7.9516
11	7.2497	6.9044	8.5408
12	8.8849	8.4286	9.2520
13	8.6243	8.2844	8.9775
14	10.8354	10.3087	12.0298
15	12.0868	10.9364	13.4835
16	6.8912	9.5067	7.3623

For better analysis, the histogram diagram for each train and test data are shown in figures 22 and 23 respectively. The sorted state based on the best average MAPE for train and test data is shown in figures 24 and 25. As figure 25 shows, in scenario 13, namely the state that data of load peak, temperature, and day type are used, the best forecast accuracy is obtained. Also, the critical point is that in conditions where only load data in the past times is used, the obtained results (last scenario) are very close to the results of the optimized scenario. This issue is because weather variables have been considered, and other variables are indirectly involved in this state. Suppose the influential variables are x_1, \dots, x_n and the desired output is modeled as the following function:

$$y = f(x_1, \dots, x_n) \tag{20}$$

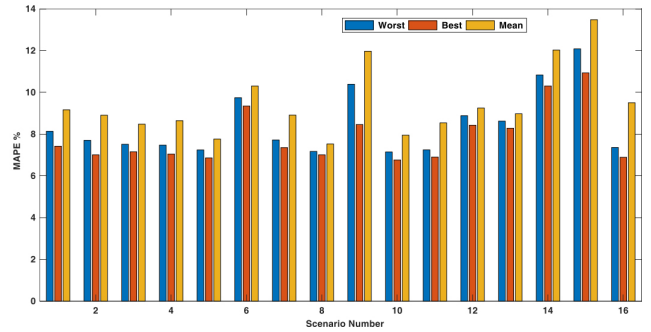


FIGURE 22. Histogram diagram for train data.

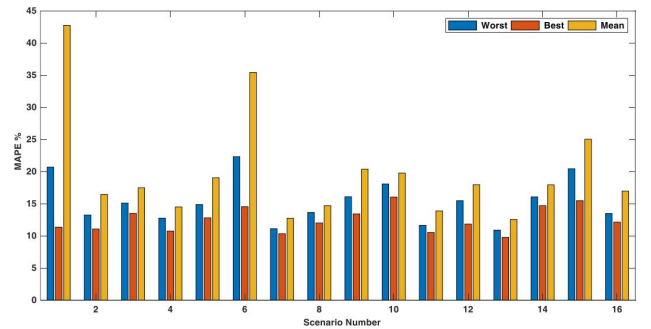


FIGURE 23. Histogram diagram for test data.

The variables x_1, \dots, x_n are valuable if we can access the value of these factors at $t + \tau$ forecast (τ is ahead of present time). In other word, the variables x_1, \dots, x_n are effective and functional when their value can be predicted well at $t + \tau$. In this problem, the desired variables are weather, economics, and population. It is impossible to predict the weather variables for long intervals of more than a few days. Especially in our regarded problem that region of study is wide, forecasting the weather variables will have many errors. As shown in simulations, other economic and population variables also have a prolonged influence. In other words, these variables affect the consumption pattern for a long period. The critical point is that when the load itself (consumption load pattern in the past times) is used as input to the problem, the other mentioned variables also are indirectly involved. In general, our model will be as follows:

$$y(t) = f(y(t-1), y(t-2), \dots, y(t-n)) \tag{21}$$

In this state, the problem inputs are variables that are themselves a function of other weather and economic and etc. variables.

IV. NEURAL NETWORK STRUCTURE OPTIMIZATION

For optimizing the NN structure (optimizing the number of neurons and layers), scenario 13 is considered, and the neuron number is changed from 10 to 100. In each case, the number of the learning iteration is considered 100. The diagrams of MAPE results for the number of different neurons for train and test data are represented in figures 26 and 27

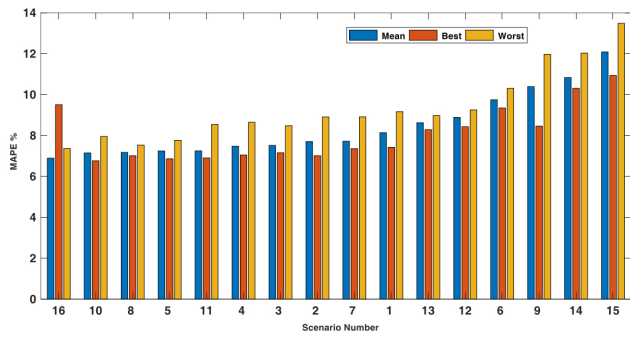


FIGURE 24. Sorting by the best average MAPE-train data.

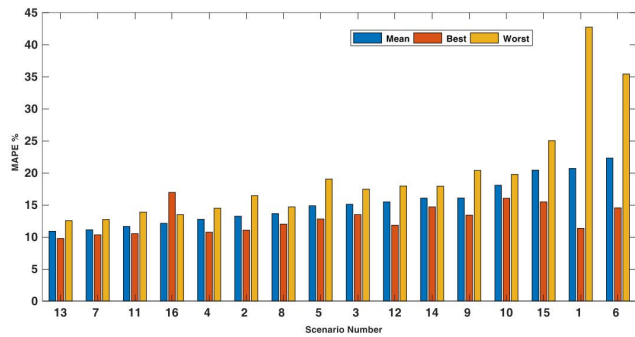


FIGURE 25. Sorting based on the best average MAPE-test data.

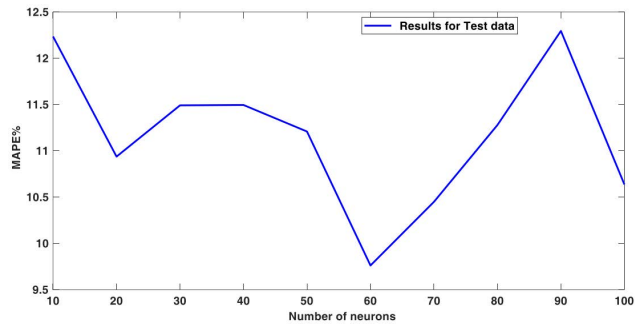


FIGURE 26. Diagram of MAPE results for the number of various neurons-test data.

respectively. As we see, by increasing the neuron numbers, the forecast system’s performance has improved. As can be seen, in 60 neurons, the best result is obtained.

V. OPTIMIZATION OF LEARNING ALGORITHM

A. THE NUMBER OF OPTIMUM ITERATION

The optimum number of iterations should be determined to avoid the overtraining problem. MAPE is calculated for both test and train data in each training iteration. At the point where the results for the test data start to rise, this point is considered the optimum training point. The results are shown in figure 28. As we see, after about 100 iterations, the results for test data are getting worse reason of which is overtraining and being fitted of coefficients to train data. In other words, after about 100 iterations, the overtraining problem happens.

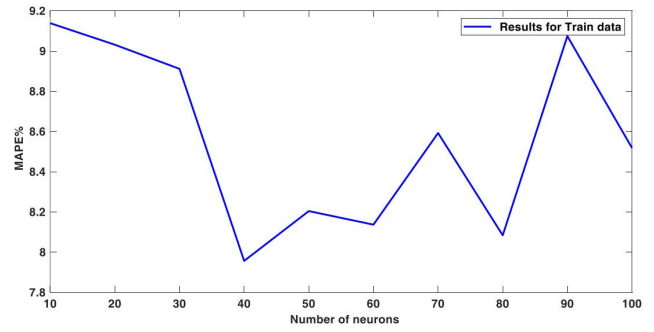


FIGURE 27. Diagram of MAPE results for the number of various neurons-train data.

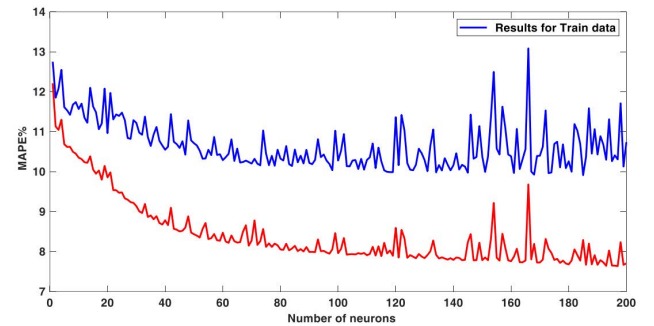


FIGURE 28. MAPE diagram in terms of number of train iteration for test and train data.

B. REDUCING THE EFFECT OF UNDESIRABLE DATA

To reduce the effect of undesired data, the Gaussian filter is considered. The undesirable data means data that has been entered wrongly due to a typo or measurement. To avoid omitting this data entirely, it is tried to reduce its effect on learning but not reach zero. Because it is not apparent whether this undesirable data is the data due to the error or the actual data that is obtained owing to some conditions, for this purpose, each input data is multiplied by a coefficient, which is considered the distance from a center. This center is considered as the average of the same days in the same month. For example, suppose the load data on Saturday, July, a year ago, enters the neural network as input. In that case, the regarded center will be considered as the average load of Saturdays in July in the past year. The training gained for this data must be reduced to reduce the destructive effect of data on learning. For this aim, we obtain the distance of each data from the average. Then, we calculate the average distance from the center. Suppose the distance related to the desired data from the average distances is more than threefold. In that case, the desired data will be considered incorrect data, and the learning rate corresponding to this data will be reduced to avoid an unfavorable effect on training.

To show the filter performance, we randomly increase the load peak two and a half times at several points. The load peak diagram, along with the filter outcomes, are depicted in figure 29. As we see, the proposed filter could recognize the insufficient data well. Also, for the state of hour-by-hour on the data related to August 2018, we doubled the load at several

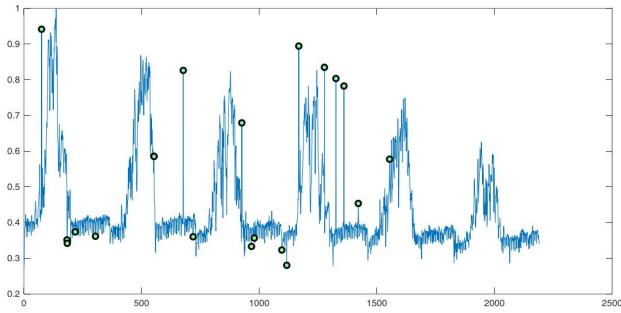


FIGURE 29. Investigation of performance of the bad-data recognition filter.

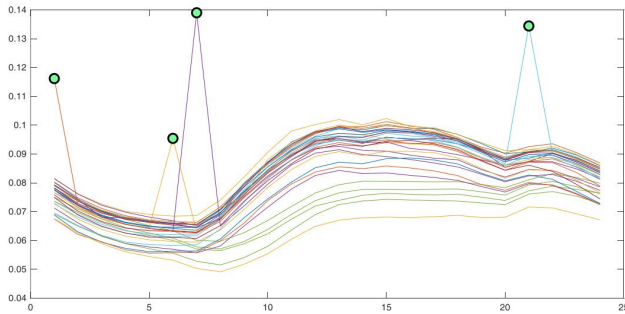


FIGURE 30. Investigation of performance of the bad-data recognition filter for the hour by hour state.

points randomly. The result of recognition is represented in figure 30. As can be seen, the proposed filter has well recognized the incorrect data. It should be noted that in the state of hour by hour, the whole day’s data is investigated hour by hour, and for each hour, a separate local model is obtained.

VI. BEST RESULTS

Previous sections examined the various scenarios to find the best practical input sets. After the most influential input sets are determined, the structure of neural networks, and the number of inputs (number of historical data), are also optimized to improve the accuracy. It should be noted that in various scenarios, accuracy is examined. For example, the best practical input sets for our data are historical load data, weather conditions, and type of day. In the following four scenarios, the effectiveness is examined. At each scenario the input sets of NN are determined.

- 1) The historical load data in the nearest similar days of the last four years (nearest in the sense of nearest date); Temperature and humidity data in the nearest similar days of the last four years; For example, if we forecast 2023, September 1, the input variables are considered as follows. Suppose that in 2023 September 1 is a working day, then in the years 2018-2022, the nearest days for September 1 are determined. Suppose the nearest working days are 2018, September 1, 2019, September 5, 2020, September 3, 2021, September 4, and 2022 September 2. Then the 15 inputs of NN are the

load peak, temperature, and humidity peaks in 2018, September 1, 2019, September 5, 2020, September 3, 2021, September 4, and 2022 September 2.

- 2) The average of 5 historical load data in the nearest similar days of the last four years (nearest in the sense of nearest date); The average of 5 temperature and humidity data in the nearest similar days of the last four years; For example, if we forecast 2023 September 1, the input variables are considered as follows. Suppose that in 2023 September 1 is a working day, then in the years 2018-2022, the four nearest days for September 1 are determined. Suppose that the nearest working days in 2018-2022 are September 1,2,3,5,8. Then the 15 inputs of NN are the average load peak, temperature, and humidity peaks in 2018-2022, September 1,2,3,5,8.
- 3) The maximum of 5 historical load data in the nearest similar days of the last four years (nearest in the sense of nearest date); The average of 5 temperature and humidity data in the nearest similar days of last four years; For example, if we forecast 2023 September 1, the input variables are considered as follows. Suppose that in 2023 September 1 is a working day, then in the years 2018-2022, the four nearest days for September 1 are determined. Suppose that the nearest working days in 2018-2022 are September 1,2,3,5,8. Then the 15 inputs of NN are the maximum load peak, temperature, and humidity peaks in 2018-2022, September 1,2,3,5,8.
- 4) The historical load data in the nearest similar days of the last four years (nearest in the sense of nearest temperature); The historical load data in the nearest similar days of the last four years (nearest in the sense of nearest humidity). For example, if we forecast 2023 on September 1, the input variables are considered as follows. Suppose that in 2023 September 1 is a working day, then in the years 2018-2022, the ten nearest days in the sense of date for September 1 are determined. Suppose that the nearest working days in the mind of date in the years 2018-2022 are September 1,...,10. The nearest days among September 1,...,10 in the sense of temperature and humidity are selected. Suppose that in 2018 September 1,...,10, the nearest day of 2023, September 1 in the sense of temperature, is 2018, September 5. Then the lead peak in 2018, September 5, is chosen as the first input data.

For examination, the load peak is forecasted for 2018 March 21 to 2019 March 21 on previous data sets from 2000 to 2017 March 20. The results for regular working days are depicted in figure 31. The simulation condition is described in Table 19, in which I represents a unit matrix. The results for all days, including working days and holidays, are depicted in figure 32.

The suggested approach applies various optimizations to get the best accuracy. In this problem, we have an extensive training data set; we need to use the most straightforward scheme. Using the other learning schemes has little impact on

TABLE 19. Simulation condition.

Inputs set	The historical load, temperature and humidity data in the nearest similar days of the last four years
Number neurons	20
Initial weights	Random between 0 and 1
η	0.5
Initial covariance matrix	$10^3 I_{n_1 \times n_1}$

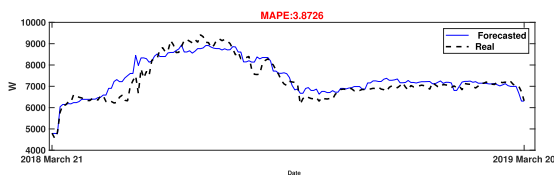


FIGURE 31. The real and forecasted trajectories for 2018 March 21 to 2019 March 20; Normal working days.

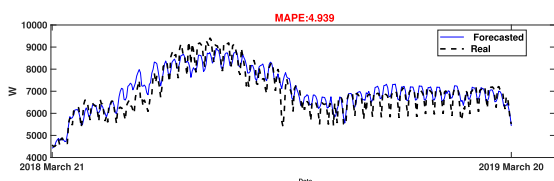


FIGURE 32. The real and forecasted trajectories for 2018 March 21 to 2019 March 20; All days including working days and holidays.

TABLE 20. The comparison of MAPE with other methods.

	Proposed Method	Recurrent NNs [37]	Deep-learned NN [30]
MAPE	3.8726	8.5141	5.4328

accuracy but imposes a substantial computational cost. For future studies, other simple and effective learning schemes can be examined.

To better show the superiority of the suggested MTLF, a comparison with some other MTLFs is presented. In [37], the recurrent NNs are developed for MTLF, and in [30] a deep-learned NN is suggested. The comparison of MAPE is given in Table 20. The Table 20 verifies that the suggested MTLF has better accuracy. It should be noted that to employ the suggested approach in other problems, all analyses should be repeated. So, using the final obtained structure in this paper may not lead to the desired accuracy. All scenarios should be repeated with new data sets to find the most effective input variables and the structure of NN.

VII. CONCLUSION

This study presents a new practical direction for MTLF. First, the influential variables and factors on accuracy are analyzed by numerical studies and computing the correlations. For numerical studies, in 16 scenarios, the inputs of NN are considered economic conditions, weather conditions,

and different social factors. The most effective and reliable inputs are selected by analyzing the various factors. Then, to improve the accuracy, the NN structure is also tuned beside the weights of NN. Also, a simple approach is suggested to detect insufficient data and decrease its impact on learning. Furthermore, to have better mid-term planning, a practical scheme is also suggested for forecasting 24-hours load patterns. The simulations by the use of actual data sets verify the applicability of the designed scheme.

REFERENCES

- [1] X. Wu, W. Zheng, X. Xia, and D. Lo, "Data quality matters: A case study on data label correctness for security bug report prediction," *IEEE Trans. Softw. Eng.*, vol. 48, no. 7, pp. 2541–2556, Jul. 2022.
- [2] L. Lin, C. Chen, B. Wei, H. Li, J. Shi, J. Zhang, and N. Huang, "Residential electricity load scenario prediction based on transferable flow generation model," *J. Electr. Eng. Technol.*, vol. 9, pp. 1–11, Jul. 2022, doi: 10.1007/s42835-022-01172-6.
- [3] X. Zenggang, Z. Mingyang, Z. Xuemin, Z. Sanyuan, X. Fang, Z. Xiaochao, W. Yunyun, and L. Xiang, "Social similarity routing algorithm based on socially aware networks in the big data environment," *J. Signal Process. Syst.*, vol. 11, pp. 1–15, Jul. 2022, doi: 10.1007/s11265-022-01790-3.
- [4] Y. Kim and S. Kim, "Forecasting charging demand of electric vehicles using time-series models," *Energies*, vol. 14, no. 5, p. 1487, Mar. 2021.
- [5] T. A. Farrag and E. E. Elattar, "Optimized deep stacked long short-term memory network for long-term load forecasting," *IEEE Access*, vol. 9, pp. 68511–68522, 2021.
- [6] B. Kermanshahi and H. Iwamiya, "Up to year 2020 load forecasting using neural nets," *Int. J. Electr. Power Energy Syst.*, vol. 24, no. 9, pp. 789–797, Nov. 2002.
- [7] B. Zhang, X. Zhao, Z. Dou, and L. Liu, "A new medium and long-term power load forecasting method considering policy factors," *IEEE Access*, vol. 9, pp. 160021–160034, 2021.
- [8] A. A. Mir, Z. A. Khan, A. Altmimi, M. Badar, K. Ullah, M. Imran, and S. A. A. Kazmi, "Systematic development of short-term load forecasting models for the electric power utilities: The case of Pakistan," *IEEE Access*, vol. 9, pp. 140281–140297, 2021.
- [9] M.-W. Tian, L. W. W. Mihadjo, H. Moria, S. Asaadi, H. S. Dizaji, S. Khalilarya, and P. T. Nguyen, "A comprehensive energy efficiency study of segmented annular thermoelectric generator; thermal, exergetic and economic analysis," *Appl. Thermal Eng.*, vol. 181, Nov. 2020, Art. no. 115996.
- [10] T.-J. Chang, S. Lee, J. Lee, and C.-J. Lu, "An interval-valued time series forecasting scheme with probability distribution features for electric power generation prediction," *IEEE Access*, vol. 10, pp. 6417–6429, 2022.
- [11] M. Ghiassi, D. K. Zimbra, and H. Saidane, "Medium term system load forecasting with a dynamic artificial neural network model," *Electr. Power Syst. Res.*, vol. 76, no. 5, pp. 302–316, 2006.
- [12] S. M. Islam, S. M. Al-Alawi, and K. A. Ellithy, "Forecasting monthly electric load and energy for a fast growing utility using an artificial neural network," *Electr. Power Syst. Res.*, vol. 34, no. 1, pp. 1–9, 1995.
- [13] D. Ko, Y. Yoon, J. Kim, and H. Choi, "Effective electricity demand prediction via deep learning," *IEIE Trans. Smart Process. Comput.*, vol. 10, no. 6, pp. 483–489, Dec. 2021.
- [14] G. Dudek and P. Pelka, "Pattern similarity-based machine learning methods for mid-term load forecasting: A comparative study," *Appl. Soft Comput.*, vol. 104, Jun. 2021, Art. no. 107223.

- [15] L. Xu, L. Hou, Z. Zhu, Y. Li, J. Liu, T. Lei, and X. Wu, "Mid-term prediction of electrical energy consumption for crude oil pipelines using a hybrid algorithm of support vector machine and genetic algorithm," *Energy*, vol. 222, May 2021, Art. no. 119955.
- [16] A. Groß, A. Lenders, F. Schwenker, D. A. Braun, and D. Fischer, "Comparison of short-term electrical load forecasting methods for different building types," *Energy Informat.*, vol. 4, no. S3, pp. 1–16, Sep. 2021.
- [17] W. Zheng, X. Liu, and L. Yin, "Sentence representation method based on multi-layer semantic network," *Appl. Sci.*, vol. 11, no. 3, p. 1316, Feb. 2021.
- [18] L. Xu, X. Liu, D. Tong, Z. Liu, L. Yin, and W. Zheng, "Forecasting urban land use change based on cellular automata and the PLUS model," *Land*, vol. 11, no. 5, p. 652, Apr. 2022.
- [19] E. E. Elattar, S. K. Elsayed, and T. A. Farrag, "Hybrid local general regression neural network and harmony search algorithm for electricity price forecasting," *IEEE Access*, vol. 9, pp. 2044–2054, 2021.
- [20] L. Peng, L. Wang, D. Xia, and Q. Gao, "Effective energy consumption forecasting using empirical wavelet transform and long short-term memory," *Energy*, vol. 238, Jan. 2022, Art. no. 121756.
- [21] H. Hassani, M. Abdollahzadeh, H. Iranmanesh, and A. Miranian, "A self-similar local neuro-fuzzy model for short-term demand forecasting," *J. Syst. Sci. Complex.*, vol. 27, no. 1, pp. 3–20, Feb. 2014.
- [22] F. Apadula, A. Bassini, A. Elli, and S. Scapin, "Relationships between meteorological variables and monthly electricity demand," *Appl. Energy*, vol. 98, pp. 346–356, Oct. 2012.
- [23] U. Amato, A. Antoniadis, I. De Feis, Y. Goude, and A. Lagache, "Forecasting high resolution electricity demand data with additive models including smooth and jagged components," *Int. J. Forecasting*, vol. 37, no. 1, pp. 171–185, Jan. 2021.
- [24] Y. Zhang, X. Shi, H. Zhang, Y. Cao, and V. Terzija, "Review on deep learning applications in frequency analysis and control of modern power system," *Int. J. Electr. Power Energy Syst.*, vol. 136, Mar. 2022, Art. no. 107744.
- [25] K. Ma, X. Hu, Z. Yue, Y. Wang, J. Yang, H. Zhao, and Z. Liu, "Voltage regulation with electric taxi based on dynamic game strategy," *IEEE Trans. Veh. Technol.*, vol. 71, no. 3, pp. 2413–2426, Mar. 2022.
- [26] L. Li, C. J. Meinrenken, V. Modi, and P. J. Culligan, "Short-term apartment-level load forecasting using a modified neural network with selected auto-regressive features," *Appl. Energy*, vol. 287, Apr. 2021, Art. no. 116509.
- [27] H. Zhang and H. Luo, "An advanced hybrid forecasting system for wind speed point forecasting and interval forecasting," *Complexity*, vol. 2020, pp. 1–16, Nov. 2020.
- [28] J. Li, S. Wei, and W. Dai, "Combination of manifold learning and deep learning algorithms for mid-term electrical load forecasting," *IEEE Trans. Neural Netw. Learn. Syst.*, early access, Sep. 3, 2021, doi: 10.1109/TNNLS.2021.3106968.
- [29] M. Khashei and F. Chahkoutahi, "Electricity demand forecasting using fuzzy hybrid intelligence-based seasonal models," *J. Model. Manag.*, vol. 17, no. 1, pp. 154–176, Feb. 2022.
- [30] B. N. Oreshkin, G. Dudek, P. Peřka, and E. Turkina, "N-BEATS neural network for mid-term electricity load forecasting," *Appl. Energy*, vol. 293, Jul. 2021, Art. no. 116918.
- [31] J.-W. Lee, K.-J. Park, J. Cho, J.-Y. Kim, and S.-Y. Son, "Novel monitoring system for low-voltage DC distribution network using deep-learning-based disaggregation," *IEEE Access*, vol. 8, pp. 185266–185275, 2020.
- [32] M. Tian, S. Yan, and X. Tian, "Discrete approximate iterative method for fuzzy investment portfolio based on transaction cost threshold constraint," *Open Phys.*, vol. 17, no. 1, pp. 41–47, Mar. 2019.
- [33] J. Benesty, J. Chen, Y. Huang, and I. Cohen, "Pearson correlation coefficient," in *Noise Reduction in Speech Processing*. Berlin, Germany: Springer, 2009, pp. 1–4, doi: 10.1007/978-3-642-00296-0_5.
- [34] X. Xu, D. Niu, L. Peng, S. Zheng, and J. Qiu, "Hierarchical multi-objective optimal planning model of active distribution network considering distributed generation and demand-side response," *Sustain. Energy Technol. Assessments*, vol. 53, Oct. 2022, Art. no. 102438.
- [35] Y. Han, S. Tan, C. Zhu, and Y. Liu, "Research on the emission reduction effects of carbon trading mechanism on power industry: Plant-level evidence from China," *Int. J. Climate Change Strategies Manage.*, vol. 7, pp. 63–77, Sep. 2022, doi: 10.1108/IJCCSM-06-2022-0074.
- [36] S. S. Haykin and S. S. Haykin, *Kalman Filtering and Neural Networks*, vol. 284. Hoboken, NJ, USA: Wiley, 2001.
- [37] S.-M. Baek, "Mid-term load pattern forecasting with recurrent artificial neural network," *IEEE Access*, vol. 7, pp. 172830–172838, 2019.

• • •